

# Spontaneous vortex arrays in a parametrically driven polariton condensate

J. O. Hamp,<sup>1,\*</sup> A. K. Balin,<sup>1,†</sup> F. M. Marchetti,<sup>2</sup> D. Sanvitto,<sup>3</sup> and M. H. Szymańska<sup>4,1,‡</sup>

<sup>1</sup>*Department of Physics, University of Warwick, Coventry, CV4 7AL, UK*

<sup>2</sup>*Departamento de Física Teórica de la Materia Condensada & Condensed Matter Physics Center (IFIMAC), Universidad Autónoma de Madrid, Madrid 28049, Spain*

<sup>3</sup>*NNL, Istituto Nanoscienze-CNR, Via Arnesano, 73100 Lecce, Italy*

<sup>4</sup>*Department of Physics and Astronomy, University College London, Gower Street, London, WC1E 6BT, UK*

(Dated: March 14, 2014)

We study theoretically a condensate of microcavity polaritons, driven resonantly in the optical parametric oscillator regime. Using a driven-dissipative generalized Gross–Pitaevskii equation, we model a finite system populated by a novel and experimentally viable pump with circular symmetry and radial currents. The resulting nonequilibrium superfluid is unstable to spontaneous symmetry-breaking and undergoes the formation of vortex arrays, which arise in the absence of any external field, potential, or rotation. The vortex arrays have nonzero net angular momentum and can rotate in one of two degenerate but chirally distinct states. This new phenomenon exists in a regime readily accessible to experiments, and we discuss possible experimental signatures of such an array.

PACS numbers: 03.75.Lm, 47.37.+q, 42.65.Yj, 71.36.+c

Macroscopically coherent quantum fluids exhibit excitations in the form of quantized vortices—topological defects in the order parameter describing the condensed phase. The ubiquity of quantized vortices has become increasingly apparent since their prediction in superfluids some decades ago [1], and they are now known to play a key role in the physics of equilibrium systems such as ultracold atomic gases, liquid helium, and type-II superconductors [2]. More recently, condensation of bosonic quasiparticles, such as microcavity polaritons [3], has been observed. Polaritons are coherent superpositions of coupled quantum well excitons and semiconductor microcavity photons. They have a finite lifetime, so their condensation is intrinsically nonequilibrium: continuous repopulation from an external source is necessary to balance photonic losses from the cavity. In the optical parametric oscillator (OPO) regime [4, 5], polaritons are resonantly injected into a pump state by a coherent laser field, before undergoing parametric scattering to signal and idler states. The sum of the phases of the signal and idler is locked by the pump, but their relative phase is otherwise free, and any explicit choice by the system breaks  $U(1)$  gauge symmetry. In this sense, though out-of-equilibrium, the OPO state can be thought of as a quantum condensate in the same way as an equilibrium Bose–Einstein condensate—both are characterized by the appearance of a Goldstone mode [6]. Recently, polariton condensates in the OPO regime have been shown to have nonequilibrium superfluid properties [7, 8], and exhibit complex and varied behavior such as spontaneous quantized vortices and persistent currents [9–11].

Vortex lattices have long been observed in rotating Bose gases [12]. Recently, similar lattices have been predicted to arise [13] in a model of an incoherently-pumped, decaying polariton condensate confined in a harmonic trapping potential, without any rotation of the trap,

so that their formation spontaneously breaks rotational symmetry. However, such lattices, with all vortices of the same vorticity and nonzero net angular momentum, have not been observed in nonequilibrium systems to date; the only observations so far have been states of vortex-antivortex pairs pinned by an external potential or the driving field [14, 15]. Experimental observation is hindered by the difficulty of engineering good quality harmonic trapping potentials which are essential for the lattice formation [16]. Also, incoherently-pumped polariton condensates are challenging to model, due to the complicated processes of pumping and thermalization, where phonons and the excitonic reservoir play important roles. The simplified model used in Ref. [13] contains constant decay and pump rates; it was further shown that vortex lattices should be robust to simple relaxation effects, i.e., frequency dependent rates [17]. However, the full influence of the reservoir and thermalization is not well understood. The OPO regime does not involve such processes, so can be easily modelled.

In this Letter we show that spontaneous vortex arrays can appear in parametrically driven polariton condensates, and this *without* the need for a trapping potential. Vortex arrays had not yet been predicted in finite OPO systems, in part since traditional pumping schemes that inject polaritons at a single wave vector  $\mathbf{k}_p$  lead to strong currents in the chosen direction [10, 18], inhibiting order. We propose and characterize a circularly symmetric polariton OPO superfluid driven with a novel and experimentally viable pump. We find that in many cases the system is unstable to spontaneous symmetry-breaking and the formation of vortex arrays. The arrays have nonzero net angular momentum and rotate in either direction, in one of two degenerate but chirally distinct states. The presence of the vortex array leads to ‘side bands’ in the photoluminescence spectrum of the system

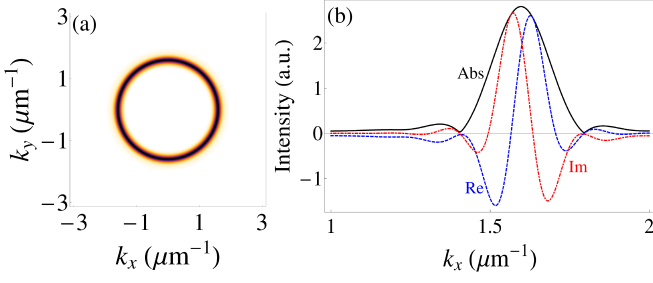


FIG. 1: External pump used to drive the system in the OPO regime. In real space the pump is given by  $F_p(\mathbf{r}, t) = \mathcal{F}_p(r) e^{i(\mathbf{k}_p \cdot \mathbf{r} - \omega_p t)}$ , with a smoothed top-hat profile  $\mathcal{F}_p(r)$ , i.e., constant radial currents of strength  $|\mathbf{k}_p|$ . (a). The absolute value of the Fourier transform of the pump field, in two-dimensional momentum space. The pump constitutes a ring of radius  $|\mathbf{k}_p|$ . (b) A cut along  $k_y = 0$ , showing the details of the ring profile in momentum space: absolute value, and real and imaginary parts.

[16], which constitutes an accessible experimental signature of such an array, in addition to possible direct imaging with time-resolved techniques. Spontaneous vortex arrays in resonantly driven polariton condensates exist as a new example of the rich phenomena associated with spontaneous pattern formation in out-of-equilibrium systems [19]. Due to their behaviour mimicking that expected in an artificial gauge field, and two-state nature which can be controlled, they have the potential to find applications in areas ranging from polaritonic devices [20, 21] to cold atoms [22].

Polaritons in a semiconductor microcavity are known to be well described by a generalized Gross-Pitaevskii (GP) equation [23] for coupled exciton ( $X$ ) and cavity photon ( $C$ ) fields  $\psi_{X,C}(\mathbf{r}, t)$  that decay with rates  $\kappa_{X,C}$  respectively, and mix with strength  $\Omega_R/2$ , where  $\Omega_R$  is the Rabi splitting between the upper (UP) and lower (LP) branches of the polariton dispersion at zero detuning. The excitonic dispersion  $\omega_X$  is taken to be the constant  $\omega_X^0$ , and the photonic dispersion is given by  $\omega_C = \omega_C^0 - \frac{\nabla^2}{2m_C}$ , where  $m_C$  is the cavity photon mass. The generalized GP equation is then (we set  $\hbar = 1$  throughout):

$$i\partial_t \begin{pmatrix} \psi_X \\ \psi_C \end{pmatrix} = \begin{pmatrix} 0 \\ F_p \end{pmatrix} + \begin{pmatrix} \omega_X - i\kappa_X + g_X|\psi_X|^2 & \Omega_R/2 \\ \Omega_R/2 & \omega_C - i\kappa_C \end{pmatrix} \begin{pmatrix} \psi_X \\ \psi_C \end{pmatrix}, \quad (1)$$

where  $g_X$  is the strength of the exciton-exciton interaction and  $F_p(\mathbf{r}, t)$  is the pump field. The traditional OPO regime is driven by a coherent continuous wave pump,  $F_p(\mathbf{r}, t) = \mathcal{F}_p(r) e^{i(\mathbf{k}_p \cdot \mathbf{r} - \omega_p t)}$ , with  $\mathbf{k}_p$  fixed in one particular direction (e.g. the  $x$ -direction), and a smoothed top-hat spatial profile  $\mathcal{F}_p(r)$  of strength  $f_p$  and full width at half-maximum (FWHM)  $\sigma_p$ . The fields  $\psi_{X,C}$  and pump strength  $f_p$  can be rescaled by  $\sqrt{\Omega_R/(2g_X)}$  so that the

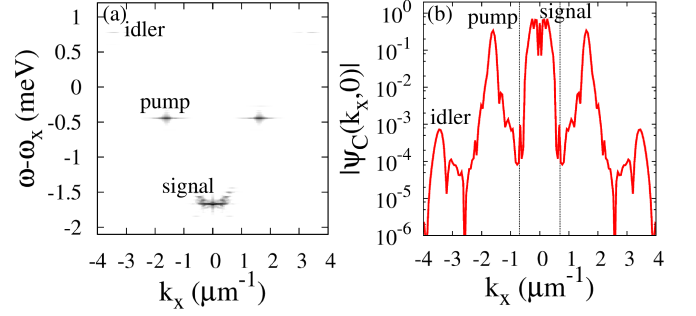


FIG. 2: (a). The full photoluminescence spectrum of the symmetric OPO system with  $\sigma_p = 35 \mu\text{m}$ , along  $k_y = 0$ . Polaritons are injected coherently into the pump state, and scatter parametrically into the signal and idler states. The intensity scale is logarithmic. (b). The momentum population of the symmetric system,  $|\psi_C(\mathbf{k})|$ , along  $k_y = 0$ . The strong occupations of the pump, signal, and idler modes as created by the OPO process can be clearly seen. Each can be obtained individually by filtering in a suitable window in momentum. The dashed lines indicate the window in which we filter to obtain the signal mode.

exciton interaction strength  $g_X$  is unity. In the present simulations we use  $m_C = 2 \times 10^{-5} m_e$ ,  $\Omega_R = 4.4 \text{ meV}$  (both typical of GaAs-based microcavities), and zero detuning. Equation (1) is solved numerically via a fifth-order adaptive-step Runge-Kutta algorithm for a system of size  $120 \times 120 \mu\text{m}^{-1}$  discretized onto  $2^8 \times 2^8$  points in space. The pump is chosen to have wave vector  $|\mathbf{k}_p| = 1.6 \mu\text{m}^{-1}$  and energy  $\omega_p = -0.44 \text{ meV}$ , in resonance with the point of inflection of the LP dispersion branch after blueshifting [24] of the polariton dispersion spectrum.

We build upon previous work in polariton OPO condensates [18] by using  $F_p(\mathbf{r}, t) = \mathcal{F}_p(r) e^{i(\mathbf{k}_p \cdot \mathbf{r} - \omega_p t)}$ , and a smoothed top-hat spatial profile  $\mathcal{F}_p(r)$ . This pumping configuration corresponds to a circularly symmetric profile, with constant radial currents given by  $|\mathbf{k}_p|\hat{\mathbf{r}}$ . The absolute value of the Fourier transform (zeroth order Hankel transform) of the pump field in two-dimensional momentum space  $|F_p(\mathbf{k})|$  can be seen in Fig. 1 (a); it is a ring of radius  $|\mathbf{k}_p|$ . The profile of the ring is shown in detail in a cut along  $k_y = 0$  in Fig. 1 (b), along with the real and imaginary parts. This pumping scheme could be realized in experiments with the aid of an axicon lens, or engineered using the phase of the laser pump, and a spatial light modulator. It leads to the generation of an OPO state that is circularly symmetric both in real and in momentum space. However, in order to investigate the dynamical stability of the symmetric system, symmetry must be broken explicitly by a small perturbation once it has reached a steady state. We use a weak probe field in resonance with the signal mode, but any other weak symmetry-breaking perturbation would work equally well. Experimentally, any small in-plane varia-

tion of the cavity field would break the symmetry. In what follows we only consider the photonic component of the polariton field since it is the quantity measured in experiments.

The full photoluminescence spectrum of the symmetric system with pump spot size  $\sigma_p = 35 \mu\text{m}$  can be seen in Fig. 2 (a) (along  $k_y = 0$ ). The generation of OPO is evidenced by the presence of signal and idler states to which polaritons injected at the pump state parametrically scatter, the signal lying at low momentum and energy, and the idler at high momentum and energy [25]. The total photonic emission in momentum space  $|\psi_C(\mathbf{k})|$  of the same system can be seen in Fig. 2 (b), as a cut along  $k_y = 0$ . Again, the macroscopic populations of the pump (at  $|\mathbf{k}_p| = 1.6 \mu\text{m}^{-1}$ ), signal (at  $|\mathbf{k}_s| \sim 0$ ) and idler (at  $|\mathbf{k}_i| \sim 2|\mathbf{k}_p|$ ) states are visible. We are interested in the behaviour of the signal mode population, which we obtain by filtering in energy or momentum, as is done in experiments. The idler has a conjugate behaviour to the signal (i.e., if vortices appear in the signal, antivortices will appear in the idler). The dashed lines in Fig. 2 (b) represent the window of  $\pm 0.7 \mu\text{m}^{-1}$  around zero momentum we use to filter out the the signal mode and obtain the signal field in real space  $|\psi_C^s(\mathbf{r}, t)| e^{i\phi_C^s(\mathbf{r}, t)}$ , where  $\phi_C^s(\mathbf{r}, t)$  is the phase of the signal wave function.

The OPO process occurs (‘switches on’) for certain ranges of detunings and pump momenta [24], only above some threshold pump strength  $f_p^{\text{th}}$ . We find the signal mode population to appear at  $f_p \equiv f_p^{\text{th}}$  and increase above threshold up to some maximum value, before beginning to disappear (‘switching off’) at around  $f_p = 1.6f_p^{\text{th}}$ . The maximum total signal intensity occurs for a pump strength of around  $f_p = 1.5f_p^{\text{th}}$ . However, the shape of the signal in real space generally becomes more complicated and less uniform on increasing  $f_p$  too far above threshold, and after symmetry breaking, the time-evolution is not stable. The regime slightly above threshold is where interesting behavior has been observed in previous work [10], and it is also the regime in which we observe steady-state vortex array solutions. We observe vortex arrays for  $1.1 \leq f_p/f_p^{\text{th}} \leq 1.25$ , and in the following use  $f_p = 1.2f_p^{\text{th}}$  unless stated otherwise. The photonic signal emission in real space  $|\psi_C^s(\mathbf{r})|$  of the symmetric system with  $\sigma_p = 35 \mu\text{m}$  and  $\sigma_p = 46 \mu\text{m}$ , can be seen in Figs. 3 (a) and (c), respectively. Superimposed are the supercurrents  $\mathbf{j}(\mathbf{r}) \equiv |\psi_C^s|^{-2} \nabla \phi_C^s(\mathbf{r})$ , determined by the interplay of pumping and decay. The dominant (radial) signal currents at nonzero  $k = 0.25 \mu\text{m}^{-1}$  have been subtracted to reveal the more complex underlying steady-state current structure which moves particles from gain- to loss-dominated regions. There are discontinuities in the current direction in the condensate, at the borders of higher- and lower-density regions.

Once the system has evolved to a steady-state regime with balanced pumping and decay, we examine dynamical

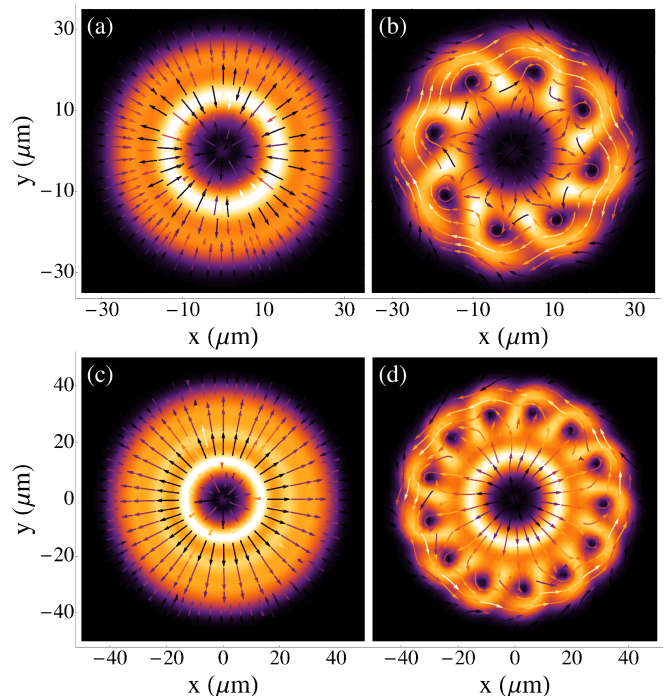


FIG. 3: The photonic component of the signal mode population of the system in real space  $|\psi_C^s(\mathbf{r})|$ . (a)-(b). With  $\sigma_p = 35 \mu\text{m}$ . (a). In the absence of a vortex array (before symmetry-breaking). (b). In the presence of an 8-(anti)vortex array. (c)-(d). With  $\sigma_p = 46 \mu\text{m}$ . (c). In the absence of a vortex array (before symmetry-breaking). (d). In the presence of a 13-vortex array. Superimposed are the supercurrents  $\mathbf{j}(\mathbf{r})$ . In the symmetric cases, the dominant signal current at small nonzero momentum has been subtracted to reveal the more complex underlying currents.

ical stability by explicitly breaking symmetry with a small perturbation. For this we add a Gaussian probe  $F_p(\mathbf{r}, t) \rightarrow F_p(\mathbf{r}, t) + F_{pb}(\mathbf{r}, t)$ , resonant with the signal mode but of much smaller dimensions ( $\sigma_{pb} \sim 3 \mu\text{m}$ ),  $10^{-3}$  times weaker than the pump, and positioned so as not to impose a preferred direction of symmetry-breaking. The strength of the symmetry-breaking perturbation influences the transitory regime but has largely no bearing on the final solution. The presence of radial steady-state currents in the symmetric system means that it is dynamically unstable to spontaneous symmetry-breaking, following which, vortices enter the condensate and can stabilize there in an ordered array. The array can be formed of either vortices or antivortices and rotates anticlockwise or clockwise (respectively), though neither sense is preferred. As such, the system spontaneously breaks circular symmetry in making a choice for the direction of rotation. The vortex array solutions are stable for extremely long times (as long as we can simulate for,  $\sim 15 \text{ ns}$ ). It remains possible to control the direction of symmetry-breaking if desired, by using a probe that imparts some momentum in one of the two possible rotation directions.

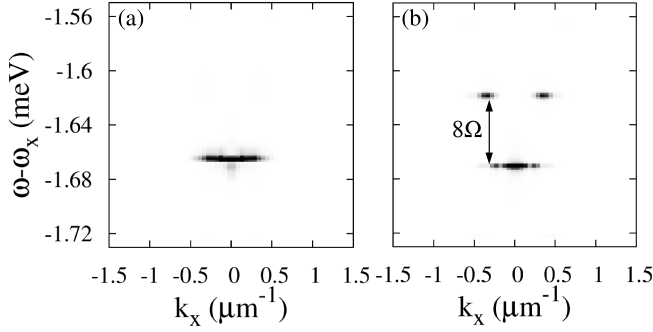


FIG. 4: The photoluminescence spectrum close to the signal mode with  $\sigma_p = 35 \mu\text{m}$ , along  $k_y = 0$ . (a) In the absence of an array (before symmetry-breaking). (b) In the presence of an 8-(anti)vortex array. In both cases the signal mode population around  $k = 0$  can be seen. In the presence of the array, two additional side-bands arising from rotation of the condensate appear, above the signal in energy by  $\Delta E = 8\Omega$ .

An example of a steady-state vortex array can be seen in Fig. 3 (b), with the supercurrents  $\mathbf{j}(\mathbf{r})$  superimposed. The system is the same as that in Fig. 3 (a). The condensate contains 8 antivortices and rotates clockwise as a rigid body with angular frequency  $\Omega = 9.91 \text{ GHz}$ . In the presence of the vortex array, taking into account the currents in the whole signal state, there are no longer discontinuous changes in the current direction throughout the condensate as in the symmetric case (see Fig. 3, (a); (c)), and the vortex array dominates the currents in the system. This 8-vortex array solution is robust to varying  $\sigma_p$  and  $f_p$  by up to around  $\pm 5 \%$ . When increasing (decreasing)  $\sigma_p$  by more than this, arrays with greater (fewer) numbers of vortices can be generated, such as the 13-vortex array in Fig. 3 (d), using a 30 % larger pump spot size (the same system as in Fig. 3 (c)). This is because vortex separation, being loosely set by the healing length, is approximately constant, so that a larger condensate can support more vortices. Outside the window of  $f_p$  values, however, the symmetry-broken system is unstable: vortices drift in and out of the condensate without ordering on the longest timescales we can simulate for. This is similar to observations in previous simulations [10]. In some cases, however, if the pump is strong enough ( $f_p \gtrsim 1.5$  over a range of  $\sigma_p$  values), and the signal population comparatively uniform, then the system can be stable to symmetry-breaking; this corresponds to when the condensate is at its most dense.

Due to rotation of the condensate, the presence of vortex arrays has been predicted [16] to give rise to ‘side bands’ in the photoluminescence spectrum, shifted in energy away from the condensate mode by  $\Delta E = n\Omega$ , where  $n$  is the number of vortices in the array. The photoluminescence spectrum near the signal (along  $k_y = 0$ ) of the system corresponding to Fig. 3 (a) is shown in Fig. 4 (a). The signal population can be seen around  $k = 0$ ,

$\omega - \omega_x = -1.67 \text{ meV}$ . The spectrum of the same system in the presence of an 8-vortex array (Fig. 2 (b)) is shown in Fig. 4 (b). Two side bands lying above the signal state can be clearly seen. The energy shift  $\Delta E$  of the side bands relative to the signal state is found to be  $0.051 \pm 0.002 \text{ meV}$ , in very good agreement with the theoretical value of  $8\Omega = 0.052 \text{ meV}$ . We find similarly good agreement in the case of arrays with different numbers of vortices. For example, for a 12-vortex array solution, we find a frequency of rotation of  $\Omega = 8.10 \text{ GHz}$ , giving a theoretical energy shift of  $12\Omega = 0.064 \text{ meV}$ , and we observe the side bands to be shifted by  $0.064 \pm 0.002 \text{ meV}$  away from the signal state. Based on our simulations, we believe that the vortex array could be directly imaged, and its rotation measured, using state-of-the-art time-resolved techniques. For example, for a 8-vortex array with  $\sigma_p = 35 \mu\text{m}$  we predict a period of rotation of 634 ps, whilst for a 12-vortex array with  $\sigma_p = 43.5 \mu\text{m}$  we predict 776 ps, which should be large enough to allow direct imaging. However, for experiments which rely upon time-integrated measurements of photonic emission, direct observation of rotating vortex arrays may be more difficult. The presence of side bands in the photoluminescence spectrum provides an alternative experimental signature of such an array. Another possible method of directly imaging a rotating vortex array in experiments using time-integrated measurements is via the defocused homodyne imaging scheme discussed in Ref. [17], which exploits the presence of the side bands in the spectrum.

To conclude, we have proposed and characterized a novel circularly-symmetric nonequilibrium polariton OPO superfluid. We find that the symmetric state can be dynamically unstable to spontaneous symmetry-breaking and the formation of vortex arrays. The arrays have nonzero net angular momentum and can rotate in either direction. Since the two possible rotation states are chirally distinct, and can be controlled, the system has the potential to find applications in polaritonic devices as a controllable two-state system i.e. bit of memory. Side bands in the photoluminescence spectrum of the system constitute an experimental signature of such an array in addition to direct imaging with time-resolved techniques. States with single spontaneous vortices in OPO superfluids have been shown to be robust to noise [10]; moreover, our vortex arrays arise in the absence of an external trapping potential, avoiding this complication altogether. This, in addition to the fact that we use parameters similar to those in current microcavity experiments, means that we expect the realization and identification of spontaneous rotating vortex arrays in parametrically driven polariton condensates to be within experimental reach.

We thank J. Keeling for helpful discussions. MHS acknowledges support from EPSRC (EP/I028900/1 and EP/K003623/1). FMM acknowledges financial support from the programs MINECO (MAT2011-22997), and CAM (S-2009/ESP-1503).

- 
- \* joh28@cam.ac.uk; Now at TCM Group, Cavendish Laboratory, University of Cambridge, J. J. Thomson Avenue, Cambridge, CB3 0HE, UK
- † andrew.balin@dtc.ox.ac.uk; Now at Systems Biology DTC, Rex Richards Building, University of Oxford, South Parks Road, Oxford, OX1 3QU, UK
- ‡ m.szymanska@ucl.ac.uk
- [1] L. Onsager, Suppl. **2**, 249 (1949).
  - [2] A. J. Leggett, *Quantum liquids: Bose condensation and Cooper pairing in condensed-matter systems*, vol. 34 (Oxford University Press, Oxford, 2006).
  - [3] J. Kasprzak et al., Nature **443**, 409 (2006).
  - [4] R. M. Stevenson et al., Phys. Rev. Lett. **85**, 3680 (2000).
  - [5] J. J. Baumberg et al., Phys. Rev. B **62**, R16247 (2000).
  - [6] M. Wouters and I. Carusotto, Phys. Rev. A **76**, 043807 (2007).
  - [7] A. Amo et al., Nature **457**, 291 (2009).
  - [8] A. Amo et al., Nature Physics **5**, 805 (2009).
  - [9] D. Sanvitto et al., Nature Physics **6**, 527 (2010).
  - [10] F. M. Marchetti, M. H. Szymańska, C. Tejedor, and D. M. Whittaker, Phys. Rev. Lett. **105**, 063902 (2010).
  - [11] G. Tosi et al., Phys. Rev. Lett. **107**, 036401 (2011).
  - [12] J. R. Abo-Shaeer, C. Raman, J. Vogels, and W. Ketterle, Science **292**, 476 (2001).
  - [13] J. Keeling and N. G. Berloff, Phys. Rev. Lett. **100**, 250401 (2008).
  - [14] G. Tosi et al., Nature Communications **3**, 1243 (2012).
  - [15] F. Manni et al., Phys. Rev. B **88**, 201303 (2013).
  - [16] M. O. Borgh, J. Keeling, and N. G. Berloff, Phys. Rev. B **81**, 235302 (2010).
  - [17] M. O. Borgh, G. Franchetti, J. Keeling, and N. G. Berloff, Phys. Rev. B **86**, 035307 (2012).
  - [18] F. M. Marchetti and M. H. Szymańska (Springer, 2012), section 6, pp. 173–213.
  - [19] M. C. Cross and P. C. Hohenberg, Rev. Mod. Phys. **65**, 851 (1993).
  - [20] M. De Giorgi et al., Phys. Rev. Lett. **109**, 266407 (2012).
  - [21] D. Ballarini et al., Nature Communications **4**, 1778 (2013).
  - [22] Y.-J. Lin et al., Nature **462**, 628 (2009).
  - [23] D. M. Whittaker, Phys. Status Solidi **2**, 733 (2005).
  - [24] D. M. Whittaker, Phys. Rev. B **71**, 115301 (2005).
  - [25] The idler state is weak, and especially so in our system since it lies on a ring of large radius in two-dimensional momentum space, and is therefore correspondingly diluted in any one-dimensional cut.